Epoxy-Montmorillonite Clay Nanocomposites: Synthesis and Characterization

Vineeta Nigam,[1] D. K. Setua,[1] G. N. Mathur,[1] Kamal K. Kar[2]

[1]*Defence Materials and Stores Research and Development Establishment, G.T. Road, Kanpur–208013, India*
[2]*Department of Mechanical Engineering and Materials Science Programme, Indian Institute of Technology, Kanpur-208016, India*

Received 8 January 2004; accepted 5 April 2004
DOI 10.1002/app.20736
Published online in Wiley InterScience (www.interscience.wiley.com).

ABSTRACT: Nanocomposites of epoxy resin with montmorillonite clay were synthesized by swelling of different proportions of the clay in a diglycidyl ether of bisphenol-A followed by *in situ* polymerization with aromatic diamine as a curing agent. The montmorillonite was modified with octadecylamine and made organophilic. The organoclay was found to be intercalated easily by incorporation of the epoxy precursor and the clay galleries were simultaneously expanded. However, Na-montmorillonite clay could not be intercalated during the mixing or through the curing process. Curing temperature was found to provide a balance between the reaction rate of the epoxy precursor and the diffusion rate of the curing agent into the clay galleries. The cure kinetics were studied by differential scanning calorimetry. The exfoliation behavior of the organoclay system was investigated by X-ray diffraction. Thermogravimetric analysis was used to determine the thermal stability, which was correlated with the ionic exchange between the organic species and the silicate layers. The morphology of the nanocomposites was evaluated by scanning electron microscopy.
 J Appl Polym Sci 93: 2201–2210, 2004

Key words: nanocomposite; epoxy resin; montmorillonite; X-ray diffraction; differential scanning calorimetry; thermogravimetric analysis; scanning electron microscopy

INTRODUCTION

Composite materials reinforced in a molecular scale are called nanocomposites and these systems have increasingly become popular. One of the most promising approaches to synthesize these materials consists of dispersing an inorganic clay mineral, in nanometer scale, into an organic polymer. Clays have long been used as filler in polymer composites because of their low cost and accomplishment of improved mechanical properties. Apart from the chemical constitution and surface characteristics, the efficiency of a filler to improve the physicomechanical properties of composites also depends on its degree of dispersion.[1] The possibility of building up a nanocomposite from polyamide (Nylon 6) and organophilic clay was first explored by researchers from Toyota.[2] Later on, other researchers also used this technique for the development of nanocomposites based on epoxies,[3,4] unsaturated polyesters,[5] polyethylene oxide,[6] polystyrene,[7] polyimide,[8] polypropylene,[9] and polyurethane.[10,11] However, meaningful separation of the clay layers could only be achieved in polymer systems, especially with the polyamide, polyimide, and the epoxy resins. A practical problem to this type of synthesis is to disperse inorganic clay in an organic medium at a molecular scale. This can be achieved by treating the clay with a long-chain alkyl amine so as to make it organophilic.[3] Once the organoclay is swollen in the monomer and the curing agent is added, complete exfoliation occurs in favorable cases. The nature of the curing agents as well as the curing conditions employed also play an important role in the exfoliation process.

Lan et al.[12] reported a balance between the intragallery and the extragallery polymerization rates that is essential to exfoliate the clay into an epoxy system. Several other different routes for the preparation of organophilic clay for different matrix systems using benzylamines, dodecylamines, and octadecylamines have been reported by Messersmith and Giannelis,[6] Zhu et al.,[13] and Bergland and Korman.[14] It is only recently that an in-depth study made by Korman[15] indicated that a long-chain alkylamine, having a chain of more than eight carbon atoms, could significantly result in an exfoliated clay structure.

In general, there are three different approaches to synthesize a reasonably good polymer–clay nanocomposite. These are as follows:

1. Melt intercalation process for thermoplastic polymers,[7]

Correspondence to: D. K. Setua (dksetua@rediffmail.com).

2. solution method, where both organoclay and polymer precursor are dissolved in a polar organic solvent,[16] and
3. an *in situ* polymerization technique.[12]

However, the *in situ* polymerization technique was found to be most effective for a thermoset polymer matrix nanocomposite.

Unique advantages of nanocomposites, which are distinctly different from their conventional counterparts, include barrier properties,[17,18] fire resistance,[19] improved mechanical properties (e.g., higher tensile modulus, tensile strength, and flexural modulus), gas impermeability, and also an increased thermal stability.[20–22] The Nylon 6–clay composite reported by Okada et al.[2] shows a major improvement in the physicomechanical properties of the composite even at a very low clay content (1.6 vol %).

Microstructure analysis using a wide-angle X-ray diffraction (WAXS) technique was used by Nair.[23] The study indicates the extent to which the layered silicate clay can be delaminated or exfoliated. Regarding the exfoliated structure, few scientists[24,25] have reported the interlamellar spacing between 90 and 110 Å and the presence of clay–polymer composite particles consisting of inhomogeneously distributed silicate aggregates within the polymer. However, multiplets of nonexfoliated layers were also observed by TEM. Researchers have also used the X-ray scattering technique for characterization of the thermoplastic–clay nanocomposites.[26–28] Chen et al.[29] and Becker et al.[30] reported on the interlayer expansion mechanism and the corresponding effect on the mechanical and morphological properties of the epoxy-based nanocomposites. The X-ray diffraction in polyimide–clay hybrid composite was studied by Yano et al.[8,31] and correlated with the basal spacing of the clay layers. Gefler et al.[32] considered poly(ethylene vinyl acetate) (EVA) and neutralized poly(ethylene methacrylic acid) (EMA) as good model systems for the understanding of the structure–property relationship and rheology of the polymer–clay nanocomposites. A series of nanocomposites prepared by EVA and EMA copolymers were characterized by DSC and small-angle X-ray scattering techniques. DSC measurement was also conducted for the Polyamide 6–clay nanocomposites by Bureau et al.[33]

Thermogravimetric analysis (TGA) of nanocomposites based on poly(dimethylsiloxane), poly(amide), and layered silicate was conducted by Wang et al.[34] and Tyan et al.[35] These studies reveal an increase of thermal stability of the composites from 25 to 60°C corresponding to a 50% weight loss. Applying the TGA method again, Doo and Cho[36] demonstrated that an intercalated polystyrene–clay nanocomposite could offer more improved thermal stability than the pristine polymer.

In this article, we report our studies on the exfoliation behavior of montmorillonite in epoxy resin nanocomposites. An aromatic diamine [diamino diphenyl methane (DDM)] was used as a curing agent in combination with a diglycidyl ether of bisphenol-A (DGEBA). The cure kinetics and the thermal stability behavior were evaluated by DSC and TGA. The microstructural analysis of nanocomposites was done by WAXS and scanning electron microscopy (SEM) techniques.

EXPERIMENTAL

Materials

The inorganic clay used, in this study, was an industrially purified montmorillonite, K-10 grade obtained from Sigma-Aldrich Co. (USA) with a cation exchange capacity of 119 meq/g. Octadecylamine was obtained from the same source. The epoxy resin taken was DGEBA with a weight-averaged molecular weight of 850 and the aromatic curing agent used was DDM. Both were obtained from the Ciba-Geigy Co. (Mumbai, Maharashtra, India). Characteristic properties of DGEBA and DDM were reported earlier.[37–39]

Preparation of inorganic composite

Inorganic clay was dried in an oven at a temperature of 75°C for 24 h. The epoxy resin was mixed with 6.0 wt % of the inorganic clay and was swelled for 3 h at 75°C. A stoichiometric amount of curing agent (27 g) was then added and mixed well. The mixture was outgassed in a vacuum oven and poured into a steel mold. It was then cured for 3 h at 75°C and postcured for 12 h at 110°C.

Preparation of organoclay

The method was similar to that used by Kawasumi et al.[40] Fifteen grams of the clay was dispersed into 1200 mL distilled water at a temperature of 80°C. Octadecylammonium chloride [$CH_3(CH_2)_{17}\ NH_3^+Cl^-$] was prepared by mixing 5.66 g octadecylamine [$CH_3(CH_2)_{17}\ NH_2$] with 2.1 mL HCl solution (10*N*) in 300 mL distilled water. It was poured into the hot clay–water mixture at a temperature of 80°C and stirred vigorously for 1 h. The mixture was then filtered and washed with water in EtOH (50/50 vol %) until no chloride was detected in the mother liquor. The octadecylamine-exchanged clay was then dried at a temperature of 75°C for 3–4 days in a vacuum oven. Thereafter, the organoclay was stored in a dessicator.

Preparation of organoclay composites

The epoxy resin was mixed with the organophilic clay, in varied proportions of 0, 1.5, 3.0, 4.5, and 6.0 wt %

TABLE I
Composition of the Nanocomposites

Nomenclature	Epoxy resin (g)	Clay (g)	DDM (g)
N_1	100	0	27
N_2	100	1.5	27
N_3	100	3.0	27
N_4	100	4.5	27
N_5	100	6.0	27

with respect to 100 wt % of the epoxy resin (as given in Table I) and was swelled for 3 h at 75°C. A stoichiometric amount (27 g) of the curing agent was then added. The mixture was outgassed in a vacuum oven and poured into a steel mold preheated at 75°C. It was then cured for 3 h at 75°C and postcured for 12 h at 110°C.

Characterization techniques

Thermal analysis

A differential scanning calorimetry (DSC) experiment was performed in a DSC 2910 instrument (TA Instruments Inc., New Castle, DE, USA). Samples were subjected to a heating rate of 10°C/min and were analyzed from ambient temperature of 30° to 350°C in a nitrogen atmosphere (flow rate, 60 mL/min).

Thermogravimetric analysis (TGA) was carried out in a high-resolution TGA 2950 (TA Instruments) over a temperature range of 30–700°C with a heating rate of 10°C/min and in the nitrogen atmosphere.

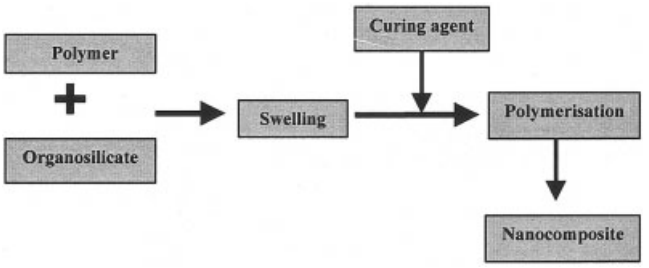

Figure 2 Flow chart presenting the different steps of *in situ* polymerization of a nanocomposite.

Determination of mechanical properties

Tensile modulus, tensile strength, and elongation at break values were evaluated by using 3-mm-thick tensile test specimens with 50 mm gauge length as per ASTM D-638 in an universal testing machine (UTM, model Instron 1158).

Wide angle X-ray scattering

WAXS equatorial scans of the composites as well as fillers were performed at room temperature (25 ± 2°C) by using a Siefert Iso-Debyeflex-2002 diffractometer [CuKα_1 radiation, λ = 1.5418 Å, 30 kV, 20 mA, step scan: 6–40° {2θ}]. The scanning speed and the step size were kept at 2°/min and 0.02°, respectively. The corrected intensity was smoothed and plotted versus 2θ. The position of the peak maximum and corresponding *d*-spacing were computed from the Bragg's diffraction equation:

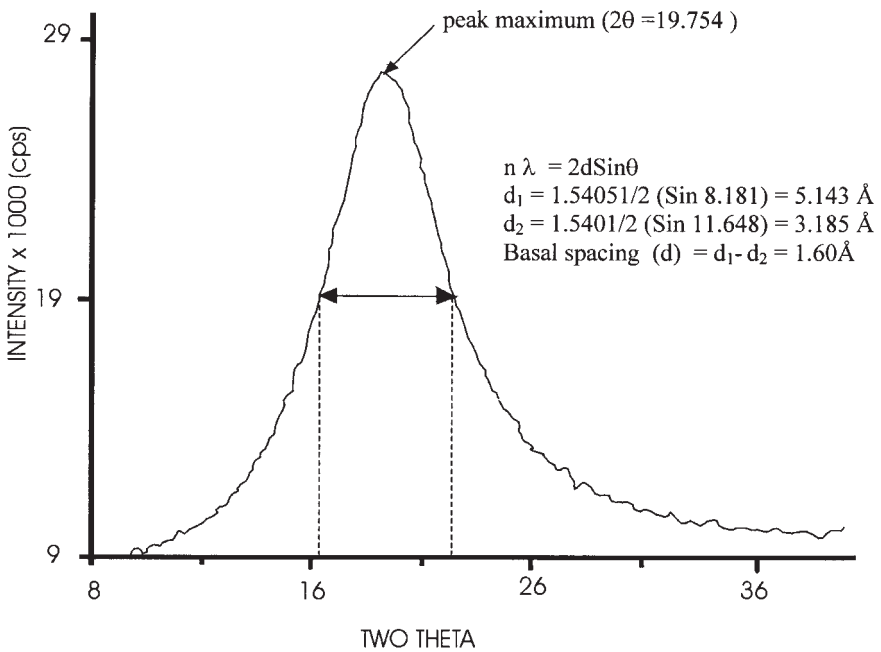

Figure 1 Sample calculation for basal spacing (d).

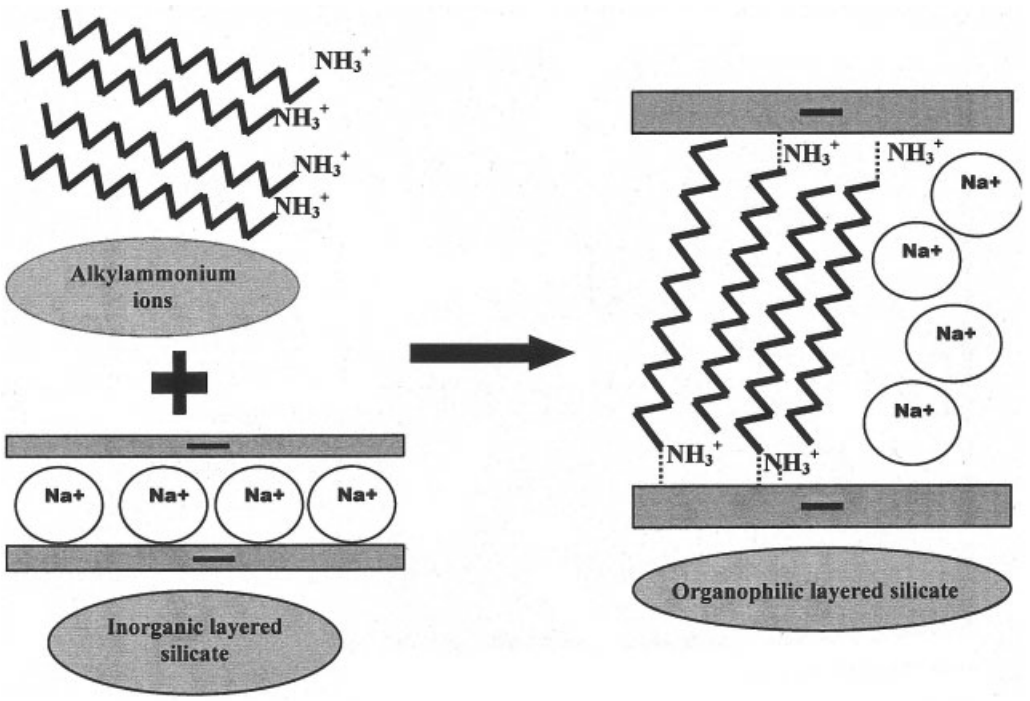

(a)

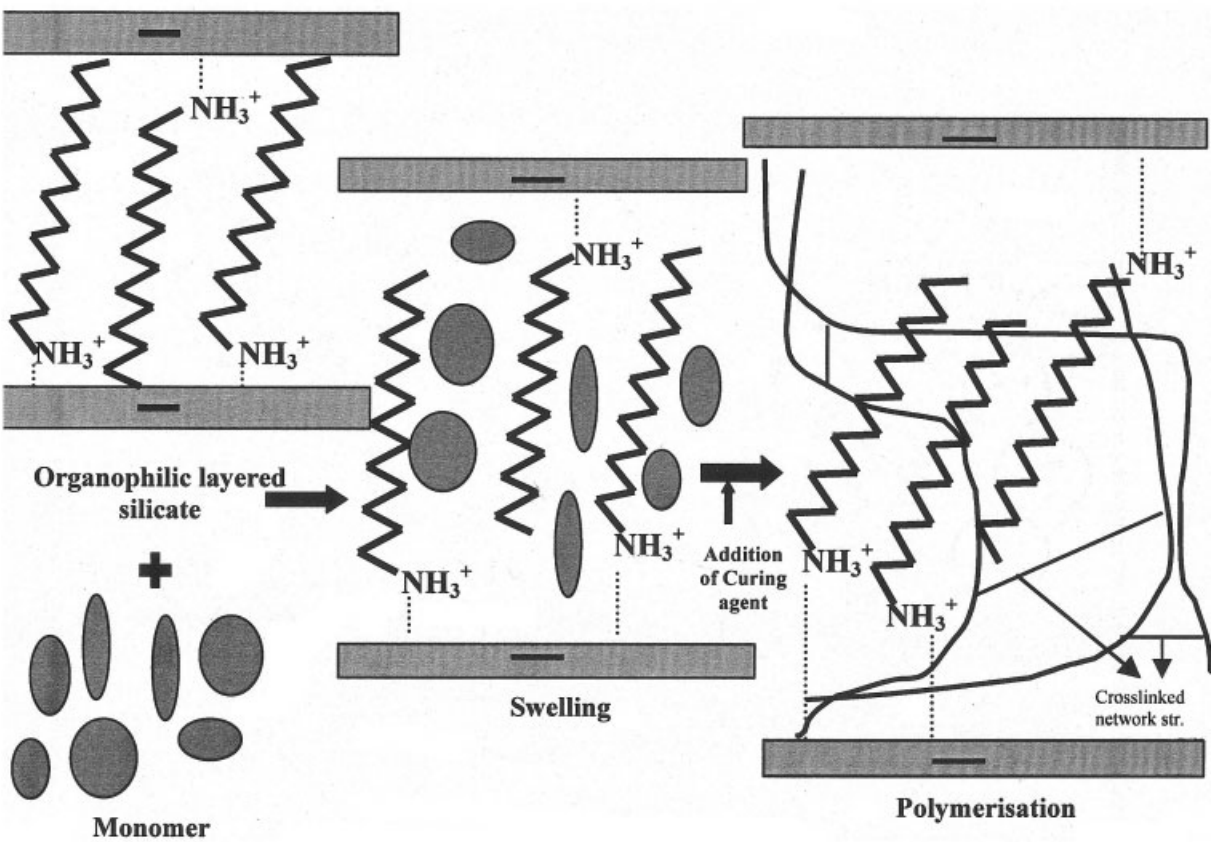

(b)

Figure 3 (a) Intercalation of layered silicate by substitution of alkyl ammonium ions for inorganic Na^+ cations. (b) *In situ* polymerization of epoxy resin by diffusion of monomer molecules between the silicate layers and subsequent crosslinking by the curing agent.

TABLE II
Differential Scanning Calorimetry Results

Mix. no.	Characteristic temperatures				Heat of reaction (ΔH) (J/g)
	T_{onset} (°C)	$T_{midpoint}$ (°C)	T_{end} (°C)	T_g (°C)	
N_1	90	165.6	260.4	70.45	430.3
N_2	87	160.9	255.0	62.23	340.0
N_3	85	157.0	252.0	60.07	335.7
N_4	82	150.2	250.0	56.69	328.9
N_5	80	148.0	245.0	53.34	323.2

$$n\lambda = 2d \sin\theta \quad (1)$$

where n is the order of reflection, λ is the wavelength of radiation, and d is the interlamellar spacing. The basal spacing for a characteristic 2θ diffraction peak, as shown in Figure 1, was obtained directly from available software. The details of this method were also reported earlier.[37,41]

SEM studies

SEM studies were performed in a JEOL JSM 35 CF scanning electron microscope. Prior to the actual SEM observation, the samples were sputter-coated with gold without touching the surface. Details of the sample preparation were earlier reported by Setua and De.[42]

RESULTS AND DISCUSSION

Fundamental principles underlying the formation of nanocomposites necessitate the monomers to migrate and react within the interlayer galleries of the layered silicate. To facilitate the intercalation, the monomer is swelled to an equilibrium stage in the layered silicate. Mixes N_2 to N_5 (Table I), containing 1.5–6% of the organoclay, were first swollen in the DGEBA resin at a temperature of 75°C for 3 h to allow complete diffusion of the epoxy precursor between the silicate layers. After addition of the curing agent, the reaction was pursued through postcuring of the nanocomposites.

Basically, the clay is a hydrophilic substance and inorganic in nature. The inorganic cation (Na^+) is required to be exchanged by a hydrophobic organic cation which also resulted in an increase of the gallery spacing. Schematic of the reaction route followed to develop the composites is given in Figure 2. The mechanism of intercalation of the organoclay and curing through the diffusion of curing agent into interspaces of the silicate galleries are depicted in Figure 3(a, b). By treating the clay with long-chain alkyl ammonium ions, the inorganic cations were replaced by the organic ones and the original hydrophilic clay was converted to hydrophobic. The epoxy chains thus could be absorbed in the intragallery spaces and pushed the layers apart. An inorganic composite was also made by using clay, at 6 wt % loading, in its original form (without any treatment) for comparison. The organically modified clay composites are termed organoclay nanocomposites.

DSC and TGA studies

The results of the DSC experiments are appended in Table II. The onset temperature of curing (T_{onset}) was found to be similar for all the compositions and in the range of 85 ± 5°C. After swelling of the organosilicate in the epoxy resin, the curing agent DDM was added. The DSC exotherms show that an increase of the organosilicate content caused a shift in the exothermal peak temperature ($T_{midpoint}$) to lower values. Perhaps the basic catalytic effect of the octadecylammonium ions on epoxy ring opening polymerization leads to a decrease of the ultimate heat of reaction (ΔH).

Figure 4 represents the plots of DSC kinetic studies on the extent of reaction versus time. Cure rate of the pristine resin was enhanced by the addition of organoclay and the rate is also progressively increased with an increasing clay content. The extent of reaction was also found to increase with time and stabilized up to

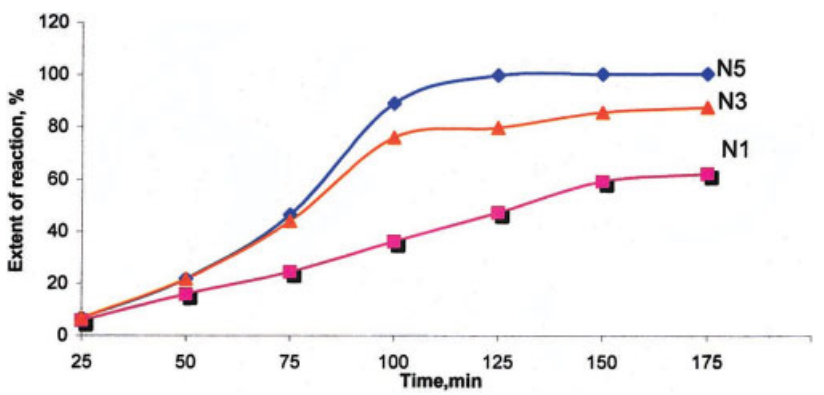

Figure 4 DSC plots of the extent of reaction versus time for the pristine epoxy resin and compositions with different clay contents.

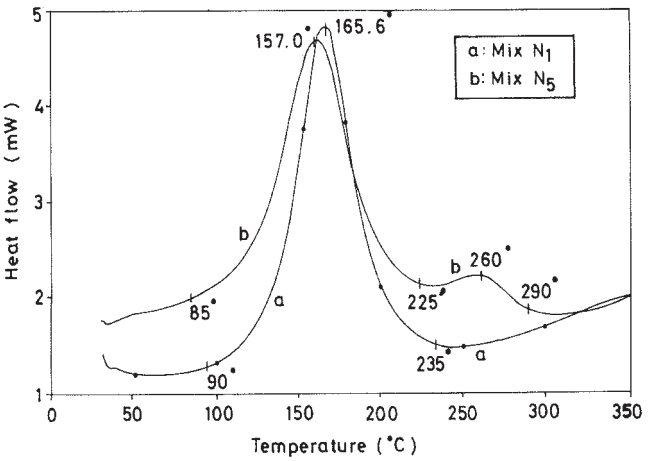

Figure 5 DSC plots of the curing of epoxy resin and the organoclay (6 wt %) filled composition, showing secondary reaction due to presence of acidic octadecylammonium ions.

3 h in all cases, which is equal to the standard cure time adopted in the preparation of the composites (both inorganic and organic). These all highlight an important prerequisite for the interlayer expansion. The alkylammonium ions have the ability to catalyze the epoxy ring opening polymerization, leading to more exfoliation and also to lowering the surface energy of the layered silicate to reduce the electrostatic interaction between the layers, thus allowing more polymer diffusion with increased organoclay content. A secondary reaction due to organic modification of clay was also evident from the DSC plots of pristine resin (Mix N_1) and 6 wt % organoclay polymer composition (Mix N_5), as shown in Figure 5.

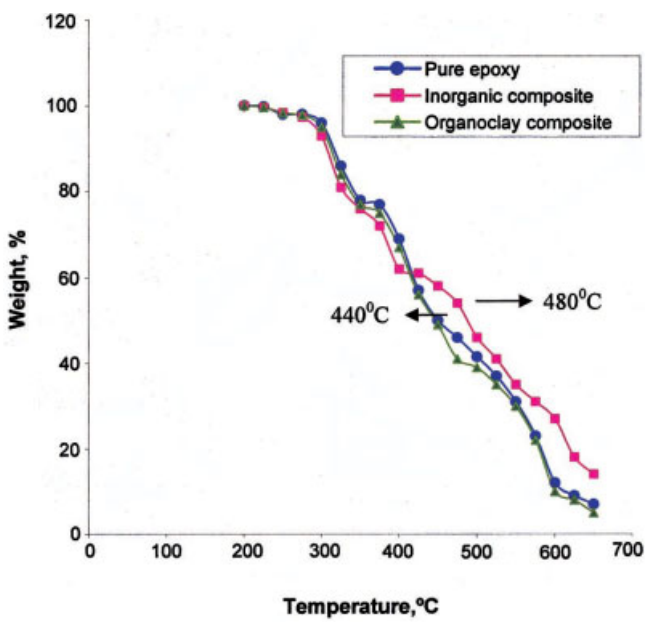

Figure 6 TGA thermograms of pure epoxy, inorganic, and organic composites.

The variations of the glass transition temperature (T_g) for the Mixes N_1–N_5 are given in Table II. A gradual decrease of T_g with increasing concentration of clay indicates that it is not an absorbed layer effect, which usually increases the T_g. Rather, the polymer chains are tied through the surface of the silicate by electrostatic interaction [Fig. 3(b)], thus reducing the surrounding entanglements. Another hypothesis concerning the decrease of T_g is that there occurs a modification of the epoxy network by its homopolymerization within the clay galleries. Indeed, if homopolymerization of the epoxy is favored between the layers, this may cause a displacement of stoichiometry in the epoxy network so that the T_g is reduced. The excess of unreacted curing agent may also plasticize the epoxy network. Due to the complexity of several possible reactions, it is difficult to determine which of these factors govern the decrease of T_g.

TGA plots for the pure epoxy, inorganic, and organoclay composites both at 6 wt % clay loadings are

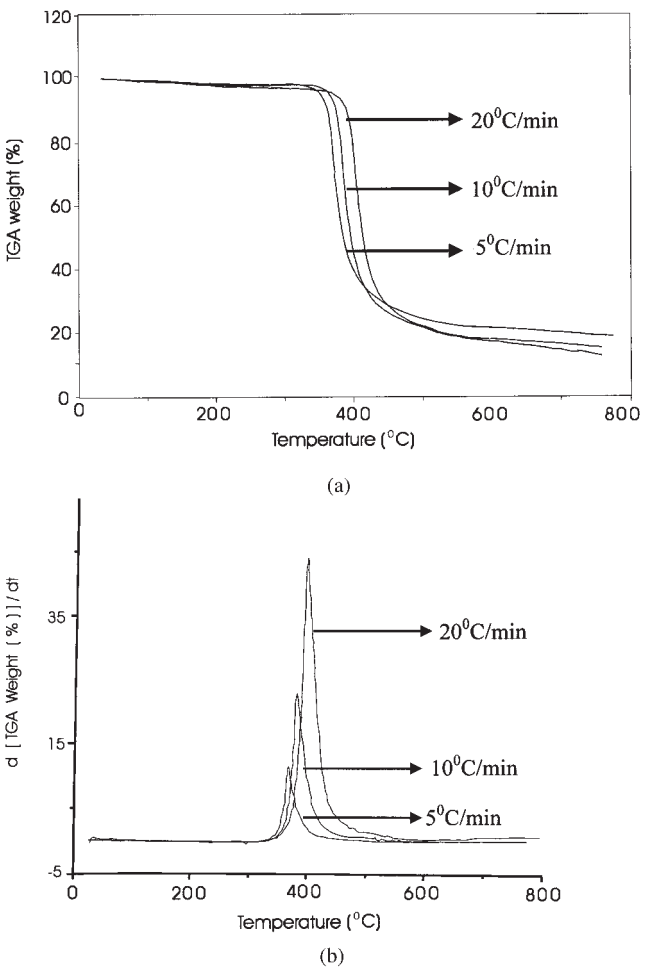

Figure 7 (a) TGA plots of organoclay composite (6 wt %) at different heating rates of 5, 10, and 20°C/min. (b) Derivative TGA plots of organoclay composite (6 wt %) at different heating rates of 5, 10, and 20°C/min.

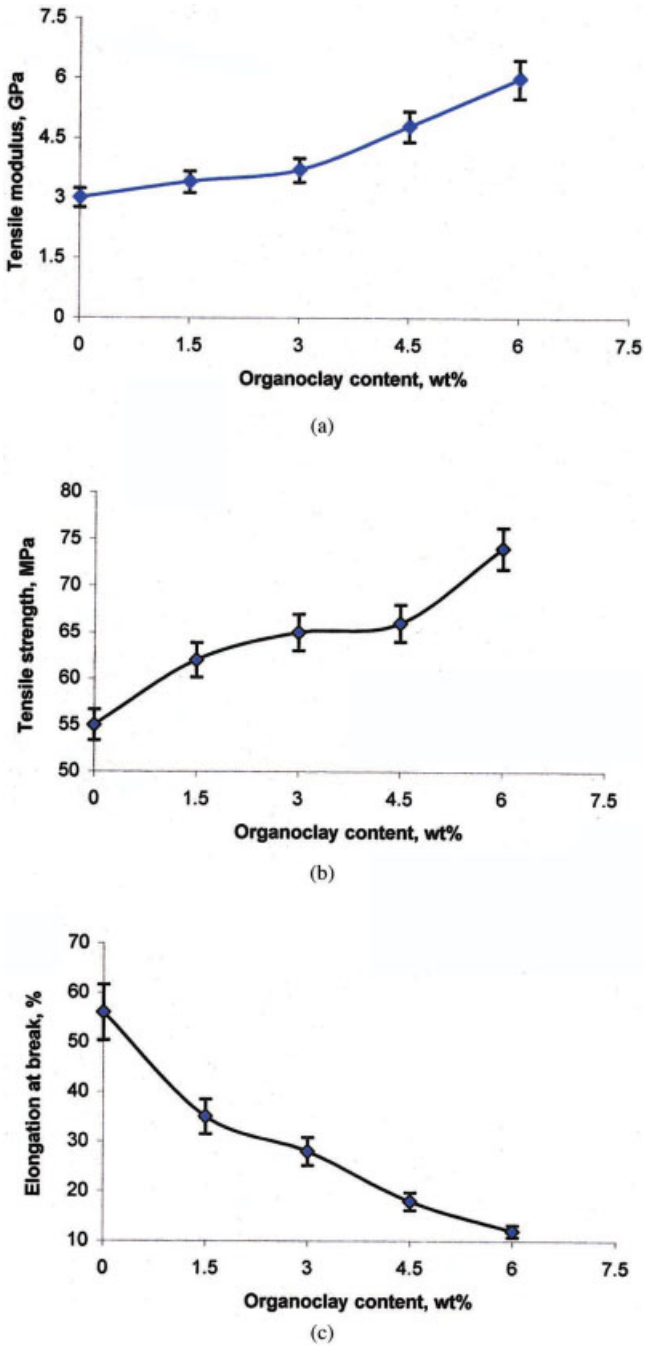

Figure 8 Mechanical properties, for example, (a) tensile modulus, (b) tensile strength, and (c) elongation at break of the nanocomposites at varied clay concentrations.

shown in Figure 6. The thermal stability of the organoclay composite appears to be less than that of the inorganic composite, as evident from the temperatures corresponding to a 50% weight loss of the individual systems. This is apparently due to lower thermal stability of the organic clay due to the presence of octadecylammonium species. Figure 7(a, b) depicts the TGA weight loss and derivative weight loss, respectively, of the 6 wt % organoclay composite at different heating rates of 5, 10, and 20°C. The plots further justify the conclusion drawn from Figure 6 (i.e., predominance of thermal stability over a less significant kinetic compensation effect).[43]

Mechanical properties

Thermosetting epoxy resins are brittle materials and can undergo only a limited plastic deformation prior to fracture.[37–39] Although deformation and cracking can both absorb the stress energy, the extent of absorption is more for the plastic deformation. At a point where the matrix deformability exceeds the critical loading, the initiation of fracture takes place.[44]

Tensile stress modulus is, therefore, one of the most important properties to study the exfoliation characteristics of the layered silicate composites. Figure 8(a–c) gives the nature of changes of the various mechanical properties of the composites with an increasing percent loading of the organoclay. A rise in the clay concentration from 0 to 6% leads to 100% increase in the tensile modulus, 20% increase in ultimate tensile strength, and 80% decrease in elongation at break values. A comparison of inorganic and organoclay composites for varied mechanical properties is given in Table III. The organoclay composite always shows better mechanical properties than the inorganic counterpart. It has also been observed that beyond a 6 wt % loading of the organoclay, the elongation at break value is lowered substantially so that a further increase of filler concentration was considered unnecessary. Beyond a 6 wt % clay loading, the inhomogeneity of filler dispersion leads to filler agglomeration and also resulted in an improper composite fabrication, which are confirmed through SEM studies described later.

Wide-angle X-ray scattering

In general, montmorillonite clay layers are approximately 1 nm thick and also possess high aspect ratio on the order of 50–1000.[5] The synthesis of exfoliated nanocomposite necessitates the clay layers to assume an efficient swelling, which leads to better dispersion. Increasing the clay content up to 6 wt % resulted in an enhancement of the mechanical properties. However,

TABLE III
Mechanical Properties of Inorganic and Organic Clay Composites

Properties	Inorganic composite	Organoclay composite
Tensile modulus (GPa)	3.6	6.0
Tensile strength (MPa)	62	70
Elongation at break (%)	25	12

TABLE IV
Basal Spacing Between the Clay Layers in the Composites

Unmodified clay composite		Organoclay composite	
2θ	d (Å)	2θ	d (Å)
19	0.8	19	50
20	1.0	20	54
22	1.2	22	70
24	1.8	24	83
26	2.4	26	87

a filler loading exceeding 6 wt % generated agglomeration of the filler aggregates to effectively reduce the available surface area of the filler. As such, the more separated the clay layers [i.e., more is the d-spacing (also known as basal or interlamellar spacing)], the better the overall mechanical properties. When the basal spacing between the layers is small (i.e., between 15 and 30 Å), the nanocomposite is termed intercalated. If the spacing is large, the nanocomposite is termed exfoliated. An increase in the basal spacing between the layers is related to an increase of the degree of exfoliation.

The values of d-spacings were obtained through X-ray diffraction (XRD) experiment and are given in Table IV. An organoclay nanocomposite always shows much higher d-spacing compared to inorganic composite for all the 2θ values considered. Figure 9 shows the XRD of the epoxy–clay composites with 6 wt % filler concentration. XRD pattern of the cured epoxy-organoclay systems exhibits a large interlamellar spacing, which indicates that the clay layers are widely separated by the curing process to form an exfoliated nanocomposite. Figure 9 and Table IV also show that, in the case of the inorganic composite, the epoxy monomers could hardly overcome the electrostatic attraction between the negatively charged silicate layers for sufficient interlayer expansion required for the formation of a nanocomposite. The XRD patterns of Na–montmorillonite pristine clay and organoclay are also shown in Figure 10 for reference.

Scanning electron microscopy

Figure 11(a, b) represents the morphology of the cross-sectional surface of the frozen (liquid nitrogen) fractured surfaces of inorganic and organoclay composites, as observed by the SEM. The bright spots on the backscattered images correspond to clay aggregates. Figure 11(a) represents the microstructure of the organoclay (6 wt %) nanocomposite where the clay particles are observed to be finely dispersed in the epoxy matrix with average size much lower than those of the conventional composite [Fig. 11(b)]. Apparently, the organoclay particles are more finely dispersed in the nanocomposite compared to the inorganic clay at equal volume loading and the difference in the degree of dispersion is due to the treatment of the clay. At higher magnification for these systems, Figure 12(a, b), we see an enhanced organophilicity of the modified clay that resulted in better matrix–filler interaction [Fig. 12(a)] than poor polymer-filler attachment coupled with failure of the polymer matrix in shear planes

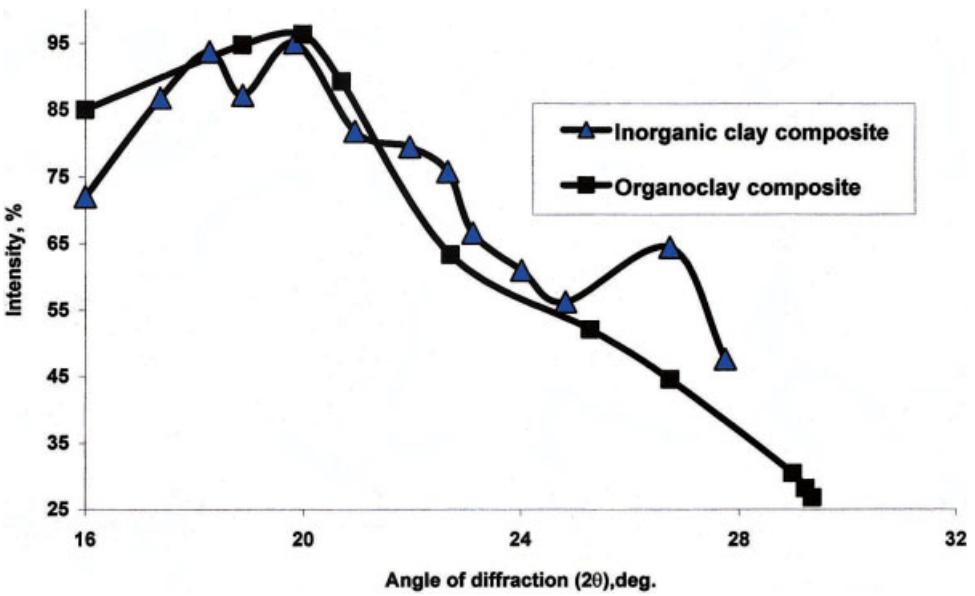

Figure 9 WAXS plots (I versus 2θ) of inorganic and organoclay composites.

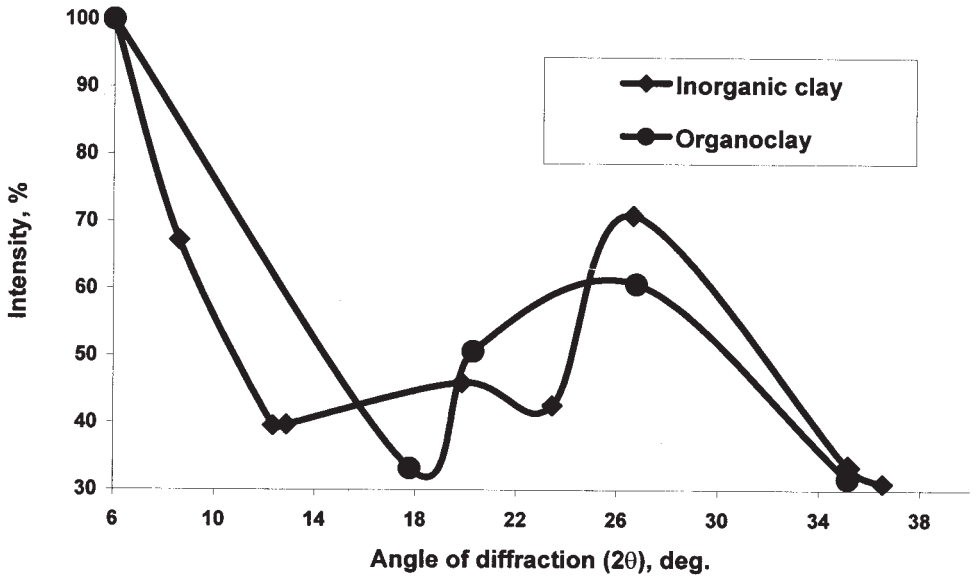

Figure 10 WAXS plots (I versus 2θ) of inorganic and organic clay fillers.

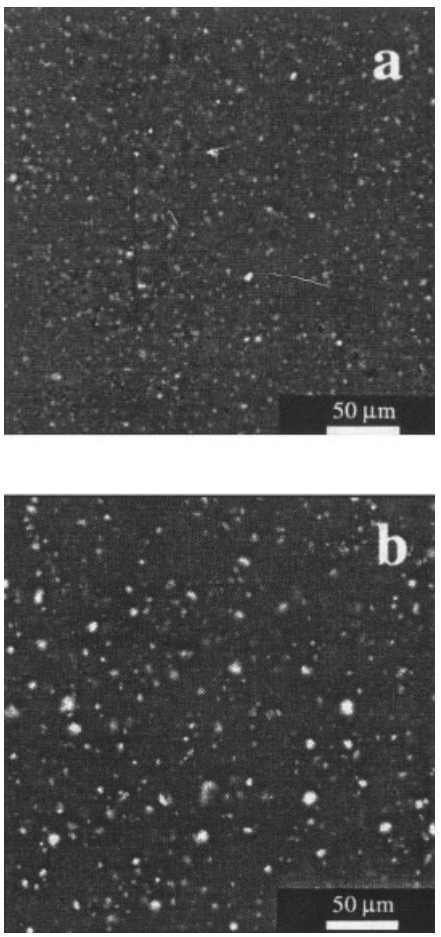

Figure 11 Scanning electron micrographs of cross-sectional surface of (a) exfoliated organoclay nanocomposite, and (b) inorganic composite.

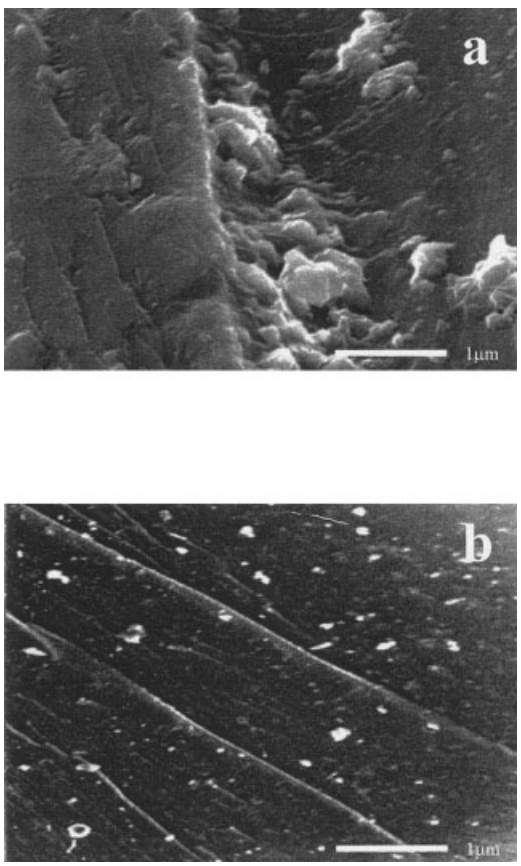

Figure 12 Scanning electron micrographs of cross-sectional surface at higher magnification of (a) exfoliated organoclay nanocomposite, and (b) inorganic composite.

[Fig. 12(b)]. Better adhesion also resulted in improved mechanical properties of the organic modified composite than those of the inorganic variety.

CONCLUSION

1. Octadecylammonium ion exchanged for Na^+ ion of pristine montmorillonite resulted in exfoliation for staggered clay galleries, which is an essential prerequisite for formation of a nanocomposite.

2. Mechanical properties of the nanocomposite attain maximum value at 6 wt % loading of the duly exfoliated organoclay. Beyond that level, the fall in mechanical properties is due to improper filler dispersion as well as the filler exceeding nanosize due to agglomeration.

3. Thermal stability of the organocomposite is less than inorganic composite. This is probably due to the presence of organic species (e.g., octadecylammonium ions), which is less thermally stable than inorganic species.

4. WAXS analysis gives insight into the mechanism of exfoliation and relative efficacy of the organic and inorganic clays.

5. SEM shows that nanocomposite has better matrix–filler interaction than inorganic composite. The studies also demonstrate a finer dispersion of the clay particles in nanocomposite as compared to the conventional composite.

6. A substantial increase (100%) in modulus and other mechanical properties of the epoxy–organoclay nanocomposites suggests an overwhelming increase of the effective volume fraction of the clay into polymer network. Such composites may attract attention to industrial sectors for structural, automotive, and packaging applications.

References

1. Theng, B. K. G. Formation and Properties of Clay-Polymer Complexes; Elsevier: Amsterdam, 1979; p. 133.
2. Okada, A.; Kawasumi, M.; Usuki, A.; Kojima, Y.; Kurauchi, T.; Kamigaito, O. Mater Res Soc Symp Proc 1990, 171, 45.
3. Messersmith, P. B.; Giannelis, E. P. Chem Mater 1994, 6, 1719.
4. Kelly, P.; Akelah, A.; Qutubuddin, S.; Moet, A. J. J Mater Sci 1994, 29, 2274.
5. Kormann, X.; Berglund, L. A.; Sterte, J.; Giannelis, E. P. Polym Eng Sci 1991, 38, 1351.
6. Messersmith, P. B.; Giannelis, E. P. J Polym Sci, Part A: Polym Chem 1995, 33, 1047.
7. Vaia, R. A.; Ishii, H.; Giannelis, E. P. Chem Mater 1993, 5, 1694.
8. Yano, K.; Usuki, A.; Okada, A.; Kurauchi, T.; Kamigaito, O. J Polym Sci, Part A: Polym Chem 1993, 31, 2493.
9. Hasegawa, N.; Kawasumi, M.; Kato, M.; Usuki, A.; Okada, A. J Appl Polym Sci 1997, 63, 137.
10. Wang, Z.; Pinnavaia, T. J. Chem Mater 1998, 10, 3769.
11. Song, M.; Hourston, D. J.; Yao, K. J.; Tay, J. K. H.; Ansarifar, M. A. J. Appl Polym Sci 2003, 90, 3239.
12. Lan, T.; Kaviratna, P. D.; Pinnavaia, T. J. Chem Mater 1995, 7, 2144.
13. Zhu, Z.; Yang, Y.; Yin, J.; Wang, X.; Ke, Y.; Qi, Z. J Appl Polym Sci 1999, 73, 2063.
14. Bergland, J.; Korman, X. Polymer 2002, 54, 1545.
15. Korman, X. Polymer 2002, 54, 1403.
16. Kawasumi, M.; Hasegawa, N.; Usuki, A.; Akane, O. Mater Sci Eng, C 1995, 6, 135.
17. Gilman, J. W.; Kashiwagi, T.; Brown, J. E. T.; Lomakin, S.; Giannelis, E. P.; Manias, E. Proc 43rd Int SAMPE Symp Part I 1998, 43, 1053.
18. Okada, O.; Usuki, A. Mat Sci Eng, C 1995, 3, 109.
19. Wang, Z.; Pinnavaia, T. J. Chem Mater 1998, 10, 1820.
20. Gilman, J. W.; Morgan, A. B.; Harris, R.; Manias, E.; Giannelis, E. P.; Wuthenow, M. in New Advances in Flame-Retardant Technology; Fire Retardant Chemicals Association, State College, PA, 1999; 9–22 pp.
21. Kojima, Y.; Usuki, A.; Kawasumi, M.; Okada, A.; Kurauchi, T.; Kamigaito, O. J Appl Polym Sci 1993, 49, 1259.
22. Yano, K.; Usuki, A.; Okada, A. J Polym Sci, Part A: Polym Chem 1997, 35, 2289.
23. Nair, S. V. Polym Eng Sci 2002, 42, 1872.
24. Korman, X.; Lindberg, H.; Berglund, L. A. Polymer 2001, 42, 1303.
25. Korman, X.; Lindberg, H.; Berglund, L. A. Polymer 2001, 42, 4493.
26. Davis, C. H.; Mathias, L. J.; Gilman, J. W.; Schiraldi, D. A.; Shields, J. R.; Trulove, P.; Sutto, T. E.; Delong, H. C. J Polym Sci, Part B: Polym Phys 2002, 40, 2661.
27. Kaempfer, D.; Thomann, R.; Mulhaupt, R. Polymer 2002, 43, 2909.
28. Gopakumar, T. G.; Lee, J. A.; Kontopoulou, M.; Parent, J. S. Polymer 2002, 43, 5483.
29. Chen, J.; Poliks, M. D.; Ober, C. K.; Zhang, Y.; Wiesner, U.; Giannelis, E. Polymer 2002, 43, 4895.
30. Becker, O.; Varley, R.; Simon, G. Polymer 2002, 43, 4365.
31. Yano, K.; Usuki, A.; Okada, A. J Appl Polym Sci 1997, 63, 2289.
32. Gefler, M.; Song, H. H.; Liu, L.; Avila-Orta, C.; Yang, L.; Si, M.; Hsiao, B. S.; Chu, B.; Rafailovich, M.; Tsou, A. H. Polym Eng Sci 2002, 42, 1841.
33. Bureau, M. N.; Denault, J.; Cole, K. C.; Enright, G. D. Polym Eng Sci 2002, 42, 1897.
34. Wang, S.; Long, C.; Wang, X.; Li, Q.; Qi, Z. J Appl Polym Sci 1998, 69, 1557.
35. Tyan, H. L.; Liu, Y. C.; Wei, K. H. Polymer 1999, 40, 4877.
36. Doo, J. G.; Cho, I. Polym Bull 1998, 41, 511.
37. Nigam, V.; Setua, D. K.; Mathur, G. N. J Appl Polym Sci 1998, 70, 537.
38. Nigam, V.; Setua, D. K.; Mathur, G. N. Polym Eng Sci 1999, 39, 1425.
39. Nigam, V.; Setua, D. K.; Mathur, G. N. Rubber Chem Technol 2000, 73, 830.
40. Kawasumi, M.; Hasegawa, N.; Kato, M.; Usuki, A.; Okada, A. Macromolecules 1997, 30, 6333.
41. Halasa, A. F.; Wathen, G. D.; Hsu, W. L.; Matrana, B. A.; Massie, J. M. J Appl Polym Sci 1991, 43, 183.
42. Setua, D. K.; De, S. K. J Mater Sci 1983, 18, 847.
43. Budrugeac, P. Polym Degrad Stab 1992, 38, 229.
44. Nigam, V.; Setua, D. K.; Mathur, G. N. J Appl Polym Sci 2003, 87, 861.